

# Channel Characterization for Underwater Acoustic Communication in the Shallow Sea-Water

Karan Shankar<sup>1</sup>, K. Saraswathi<sup>2</sup>

<sup>1</sup>Student, Master of technology, Department of Electronics & Communication Engineering, RVCE, Bengaluru, Karnataka, 560059, India

<sup>2</sup>Assistant Professor, Department of Electronics & Communication Engineering, RVCE, Bengaluru, Karnataka, 560059, India

**Abstract:** *This paper is intended to model the communication channel which is sea-water for the propagation of the acoustic signals. The shallow water experiences lots of turbulence due to high-speed winds blowing on the sea, which leads to breaking of the waves and thus formation of cloud bubbles. These bubbles are responsible for the variations in the sound speed profile causing potential attenuation in the signal strength, which is again dependent on the depth below the sea-surface. Thus, as the depth increases the bubble size and the density decrease. This distribution of the bubble plumes model the channel and their effect is dominant in rough sea-surface. The bubble model by Norton et al., is used to give the parabolic distribution of the bubble size and density depending on the wind speed and depth below the surface. This model thus can be used to obtain the frequency response of the non-uniform channel, and so scattering due to bubble plumes is major cause for attenuation.*

**Keywords:** bubble plumes; temperature gradient; diffusion

## 1. Introduction

Shallow sea water offers great challenge to acoustic signal propagation. The sea-water is assumed to be a uniform medium separating air and water. This is not very true in real sense when other factors are accounted for like the effect of the presence of the wind blowing with high speed over the surface, the various dead and living components and finally the micro particles. All these make the so called uniform waveguide into a highly disturbed medium. This perturbation is the cause of the attenuation experienced by the acoustic signals mainly in the range of 2-4 KHz for our purpose.

The main cause for attenuation of the acoustic signal is the scattering of the signal due to heterogeneous nature of the channel due to the presence of broken waves which decompose into cloud of bubbles, the dissolved sand and other particles. The effect of the bubble plumes are the cause for scattering of the signal rather than the refraction. Some of the bubbles being comparable to the wavelength of the acoustic signal which results in the scattering due to the Doppler shift of the various frequency components. These phenomena affect the high frequency signal more than the low frequency signals.

Series of papers published by G. Norton, J. Novarini, and R. Keiffer [1],[2] have witnessed the effect of the bubble plumes on the frequency of the acoustic signal on the 2-4 KHz range, though the effect can be witnessed for many high components of the signal. They have developed a model which is based on the measurements taken from Martha's Vineyard Coastal Observatory. The model in [2] discussed by Novarini and Norton concentrate on the discrete model of the bubble plumes because the plumes vary on the range and the depth. The sea-surface model by Elfouhaily [3] et al., can be used to generate the sea surface spectra. With bubble distribution the sound speed relation is highly distributed along the surface and below it. The following steps can be used like, firstly generalization of the

surface with the Fourier transform followed by the surface nature estimation based on the previous model.

The surface being very dynamic can be modeled by keeping the bubble perturbed sound speed profile constant. Going for each depth part we can obtain the full behavior to few meters below the surface.

### A. Bubble plumes model

In shallow sea-water acoustics experiences the compact assemblages of bubbles which are usually referred to as *clouds* or *plumes* without any distinction. S. A. Thorpe [11], was among the firsts to describe these compact population of bubbles, and thus used the term "clouds" and made the distinction between two types of clouds depending on the interaction with the windy air: the bubble clouds, which occurs when the air temperature exceeds water temperature, and *columnar* clouds, occurring when the water temperature exceeds air temperature. Reference [3] gives clear distinction between the plumes and clouds and describes the clouds or plumes superimposition on the "near to surface bubble layer." He also stated that "the plumes appear in a roughly v-shaped, which decreases in width with depth." This provides a clear understanding for Thorpe's columnar clouds and the definition of the word "plume" (which refers to feather-like structure). Adopting the word plume represents v-shaped columnar clouds and use cloud as a generic term to refer to any compact aggregate (patch) of micro-bubbles. Based on the observations made in [10] we have three types of bubble plumes namely  $\alpha$ ,  $\beta$  and  $\gamma$  where two of them are present in the stages of whitecaps: stage A and B, which are associated with the crests and the foam patches where  $\alpha$ -plumes is the initiation phase of the stage A whitecap. They have the highest void fraction of  $O(10^{-1}-10^{-2})$  and are very small in size and have a very short lifetime (<1s). The  $\alpha$ -plumes transforms into a  $\beta$ -plume after some time when the momentum of the cloud gets downwards. Thus, the stage A whitecap transforms into a foam patch i.e. stage B. The void fraction of  $\beta$ -plumes is much smaller typically  $O(10^{-3}-10^{-4})$  which are attached to the foam patch.

That is, the stage B whitecap is the top of the  $\beta$ -plume. The  $\beta$ -plumes are much bigger than the  $\alpha$ -plume and also have longer lifetimes (about 4 s). This transformation continues and the  $\beta$ -plumes then evolve into  $\gamma$ -plumes and get separated from original whitecap. This newly generated  $\gamma$ -plume has lower void fraction of ( $10^{-6}$ - $10^{-7}$ ) with huge dimensions, and greater lifetimes (10-100 times longer) compared to the  $\beta$ -plumes. After some time  $\gamma$ -plume decays to form the background. The  $\beta$ -plumes and the  $\gamma$ -plumes can be recognized as conical structure with cross-sections that decrease exponentially with increasing depth, as stated in [3]. A cartoon sketch of the different plumes is shown in Fig. 1. The  $\alpha$ - and  $\beta$ -plumes are respectively accompanied by type A and B whitecaps.

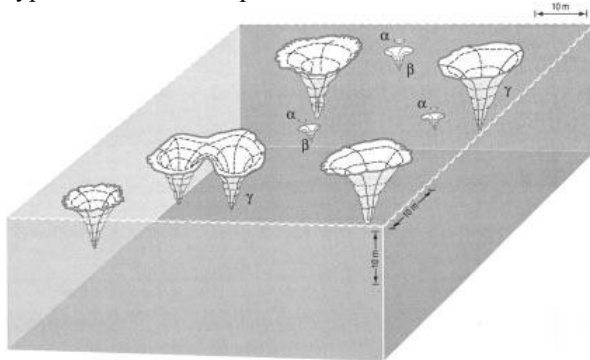


**Figure 1:** Bubble plume at different stage of development ( $\alpha$ -plume,  $\beta$ -plume, and  $\gamma$ -plume).

As stated in [10], the shape of the different stages in the development process of plumes, the  $\beta$ -plumes,  $\gamma$ -plumes are almost identical to each other which is also discussed in [12]; though they differ in the void fraction, bubble shape, spectral amplitude. Following the parameters discussed in the references [5],[7],[11], the bubble population of each type can be represented by general function as:

$$n(a, z, u) = N_0 G(a) Z(z) U(u) \quad (1)$$

where  $a$  being the radius of the bubble,  $z$  being the depth below the surface, and  $u$  being the wind speed at 10 meters above the water. Let's get to obtain the similar equation for the  $\beta$ -plumes,  $\gamma$ -plumes, and the bubble layer present in the background. As stated in reference [11], the rate of generation of plumes and the whitecap is equal, which is proportional to the fraction of the sea surface instantaneously covered by whitecaps (similar to Monahan's stage B) and happens to be the function of speed of the winds. Monahan in [13] could also infer that the fraction of the sea surface instantaneously covered by whitecaps is directly proportional to the cube of the wind speed and friction velocity. As all the bubbles are assumed to be generated by wind, the function  $U(u)$  will remain same for all the stages of plume development. As stated in [4], the estimated form is

$$U(u) = (u/13)^3 \quad (2)$$

The function of the Spectral shape can taken to be

$$G(a) = \begin{cases} 0 & a < a_{min} \\ \left(\frac{a}{a_1}\right)^3 & a_{min} \leq a < a_1 \\ 1.0 & a_1 \leq a < a_2 \\ \left(\frac{a_2}{a}\right)^4 & a_2 \leq a < a_3 \\ \left(\frac{a_2}{a}\right)^4 \left(\frac{a_3}{a}\right)^{2.6} & a > a_3 \end{cases} \quad (3)$$

Where  $a_{min} = 10\mu\text{m}$ ,  $a_1 = 15\mu\text{m}$ ,  $a_2 = 20\mu\text{m}$ , and  $a_3 = 54.4 + (1.984)z$ , with  $a_3$  in micrometers and  $z$  in meters.

### B. The $\beta$ -plumes

The  $\beta$ -plumes are present at 0.25 meters below the sea-surface which is the result of the breaking waves and has the highest concentration at that level as also stated in [13],[14]. Fig.2 shows the population of the bubbles at 0.2 meters below the surface at different wind-speed, as clearly given in the graph, the bubble are generated with high wind speeds. The spectral slope of the bubbles in the radii range of 30 to 50 meters is -4 and for bubbles larger than 60 meters it is -2.6. According to the Wu hypothesis the change in the spectrum is from 2 to 4 as the cloud moves away from the sensors.

population vs radius graph of Beta plume at 0.2 meter depth and different wind speeds

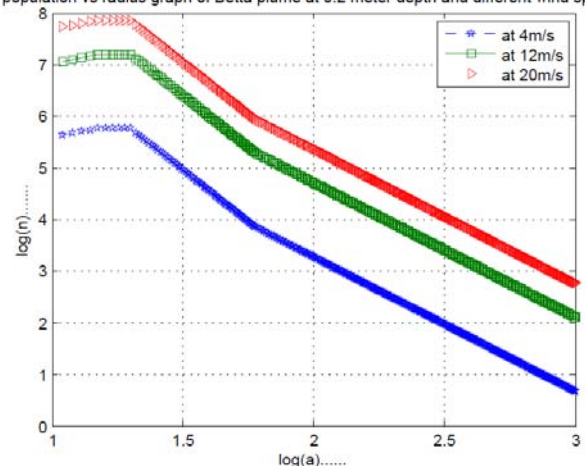


**Figure 2:** Bubble spectra for the  $\gamma$ -plumes and a  $\beta$ -plume at  $z = 0.25$  meters, wind speed 13 m/s.

Taking the aspects discussed in the reference [13], and the idea that the spectral slope lies in the range of -2 to -4 when the depth increases, the findings state that this swing is from -2.5 to -4 instead which occurs rapidly with depth change concluding on these findings, the adopted value of -2.6 for the spectral slope of the  $\beta$ -plumes for bubble larger than  $60\mu\text{m}$  and smaller than  $a_{max}$ . The spectral shape can be seen as

$$G_{\beta}(a) = \begin{cases} 0 & a < a_{min} \\ \left(\frac{a}{a_1}\right)^3 & a_{min} \leq a < a_1 \\ 1.0 & a_1 \leq a < a_2 \\ \left(\frac{a_2}{a}\right)^4 & a_2 \leq a < a_3 \\ \left(\frac{a_2}{a_3}\right)^4 \left(\frac{a_3}{a}\right)^{2.6} & a > a_3 \end{cases} \quad (4)$$

Making the assumption that the larger bubbles are found at the and as the depth increases, these bubbles shrink and get extinct gradually. Wu in [11] showcased a plot of the maximum possible radius of the bubbles as a function of increasing depth, which is given by

$$a_{\max}(z) = a_{\max}(z=0) \exp(-z/4.1) \quad (5)$$

Bubble with radii exceeding  $a_{\max}$  do not form the final spectrum. Note that in some cases  $a_{\max}$  may become smaller than  $a_3$ . For  $\beta$ -plumes, the bubble spectral density is given by

$$n_{\beta}(a, z, u) = N_{0, \beta} G_{\beta}(a) Z_{\beta}(z) U_{\beta}(u) \quad (6)$$

The function  $Z_{\beta}(z)$  is the variable causing the change in the vertical length of the plumes axis. So concluding from [13] the distribution of the bubble with the depth is given by,

$$Z_{\beta}(z) = \begin{cases} 1 & z \leq Z_{\beta \max} \\ 0 & z > Z_{\beta \max} \end{cases} \quad (7)$$

Where,  $z_{\beta \max}$  is the maximum depth. The  $\alpha$ -plumes get transformed into  $\beta$ -plumes due to the waves thus the maximum depth is proportional to the motion of the waves. From Johnson's reference [12], it can be inferred that the  $\beta$ -plumes are present till one half of the significant wave height ( $H_{1/3}$ ). Since  $H_{1/3}$  is multiple with four times the rms roughness, the maximum penetration of the  $\beta$ -plumes is thus,

$$Z_{\beta \max} = (1.23 \times 10^{-2}) u^2 \quad (8)$$

The constant of  $N_{0\beta}$  (6) is taken such that it results to values within the range specified by Monahan for the bubble density about the concentration, void fraction of the  $\beta$ -plumes. Setting  $N_{0\beta}$  equal to  $2 \times 10^7$  ( $m^{-3} \mu m^{-1}$ ) leads to a spectral density of ( $a=100 \mu m$ ) =  $1.1 \times 10^{-5}$  ( $m^{-3} \mu m^{-1}$ ) and void fraction of (0.08%), at the surface at the wind-speed of 15 meters/second.

The horizontal cross-sectional area of the plumes changes with the depth and inferring from the reference [10], the  $\beta$ - and  $\gamma$ - plumes have the same characteristics.

$$A(z) = A_0 e^{(-z/d)} \quad (9)$$

Where  $A_0$  being plumes area ( $m^2$ ) at the plumes surface and  $d$  being any constants.

In case of the  $\beta$ -plumes, the area of the type B foam patch determined the size of the plumes at the sea-surface. The estimated area of the type B foam (in  $m^2$ ) would be:

$$A_{0\beta} = 17.0 + 0.0307(u-5)^2 \quad (10)$$

The area's square-root is the length of the plumes.

$$L_{\beta}(z) = L_{0\beta} e^{(-z/Zd\beta)} \quad (11)$$

Where  $L_{0\beta} = L(z=0) = (A_{0\beta})^{1/2}$ . At the maximum penetration depth for the  $\beta$ -plumes ( $Z_{\beta \max}$ ), Lets take that  $L_{\beta}(z = z_{\beta \max}) / L_{0\beta} = 0.05$ . Thus, the constant  $d_{\beta}$  in (11) being

$$d_{\beta} = \frac{Z_{\beta \max}}{5.99} \quad (12)$$

The distribution in the range of the Plumes is required to completely give the description of the  $\beta$ -plume. Assuming the [10] inputs where the  $\beta$ -plumes are attached to the type B

whitecaps (foam patches), the spacing  $S_{\beta}$  in meters) between  $\beta$ -plumes is set equal to the spacing between foam patches, which is given by

$$S_{\beta} = (237) u^{-1.07} \quad (13)$$

### C. The Sound Speed profile and variations in the Bubble Spectral density

The compressing ability of the mixture is dependent on the change in compressibility of ( $\Delta K$ ), the substitution in the Wood's equation results into the equation.

$$K = (1 - V) K_0 + \Delta K \quad (14)$$

Where  $K_0$  is the compressing ability of the water when no bubble is present,  $V$  is the volumes occupied by bubble. For  $\Delta K$ , considering that water containing  $N$  bubbles per unit volume, with each radius  $a$ , and assuming  $ka < 1$ . This expression can be rewritten as

$$\Delta K(f, z) = \frac{N a}{\rho \pi f^2 \left( \frac{f_r}{f} - 1 + i\delta \right)} \quad (15)$$

Where  $\delta$  is the damping constant and  $f_r$  is the resonant frequency.

$$\Delta K(f, z) = \frac{1}{\rho \pi f^2} \int_{a_{\min}}^{a_{\max}} \left[ \frac{an(a)}{\left( \frac{f_r}{f} \right)^2 - 1 + i\delta} \right] da \quad (16)$$

The response frequency is based on the thermal conditions and tensile pressure on the surface. With the assumption that there are adiabatic oscillations, and ignoring the viscous effect, the resonant frequency of the bubble having radius  $a$  (in  $\mu m$ ) can be given by

$$f_r = \sqrt{\left( 1 + \frac{z}{10} \right)} (3.25 \times 10^6) \frac{1}{a} \quad (17)$$

$\delta$  comprises of :  $\delta_r$  is due to radiation;  $\delta_v$  i.e. shear viscosity, and  $\delta_t$  i.e. thermal conductivity:

$$\delta = \delta_r + \delta_v + \delta_t \quad (18)$$

The radiation component is given by:

$$\delta_r = 2 \pi f a / C_0 \quad (18.1)$$

Where  $f$  = frequency in Hz, and  $C_0$  is speed of sound in water, assumed 1.5 km/s.

The  $\delta$  due to diffusion of heat is:

$$\delta_t = 3 \text{Im}g(B) / \rho \omega^2 a^2 \quad (18.2)$$

$\rho$  is the density of water taken as 999.9720 kg/m<sup>3</sup>

$$B = \frac{\gamma P_0}{1 - \left[ \frac{3i(\alpha-1)}{2\phi^2 a^2} \right] \{ (1+i)\phi a \cot[(1+i)\phi a] - 1 \}} \quad (19)$$

Where  $P_0$  is the hydrostatic pressure at the bubble given by

$$P_0 = P_A + \rho g z \text{ (Pa)}, \quad (20)$$

$$P_A = 101325 \text{ (Pa)} \quad (20.1)$$

$$g = 9.8 \text{ m/s}^2, \gamma = 1.4, D = 1.84 \times 10^{-5} \text{ (m}^2/\text{s)} \text{ and, } \varphi = \sqrt{\omega/2D}$$

The complex effective sound speed is given by

$$C_{\text{eff}}^{-2} = [(1-V) \rho + V \rho_{\text{gas}}] [(1-V) K_W + \Delta K] \quad (21)$$

Since  $\Delta K$  is a complex number,  $(C_b)$  provides the phase velocity and  $\text{Im}g$  part gives the attenuation due to bubble.

$$C_b = \text{Re} \{ C_{\text{eff}} \} \quad (22)$$

$$\alpha_b \text{ (dB/m)} = \frac{20 \text{ Im}g \{ 1/C_{\text{eff}} \}}{\ln(10)} \quad (23)$$

For low void fractions ( $V \gg \rho_{\text{gas}}/\rho$ ), (19) can be simplified to

$$C_{\text{eff}}^{-2} = C_0^{-2} + \rho \Delta K \quad (24)$$

Replacing  $\Delta K$  from (15) to (22)

$$C_{\text{eff}}^{-2} = C_0^{-2} + \frac{1}{\pi f^2} \int_{a_{\text{min}}}^{a_{\text{max}}} \left[ \frac{a n(a)}{\left(\frac{f r}{f}\right)^2 - 1 + i\delta} \right] da \quad (25)$$

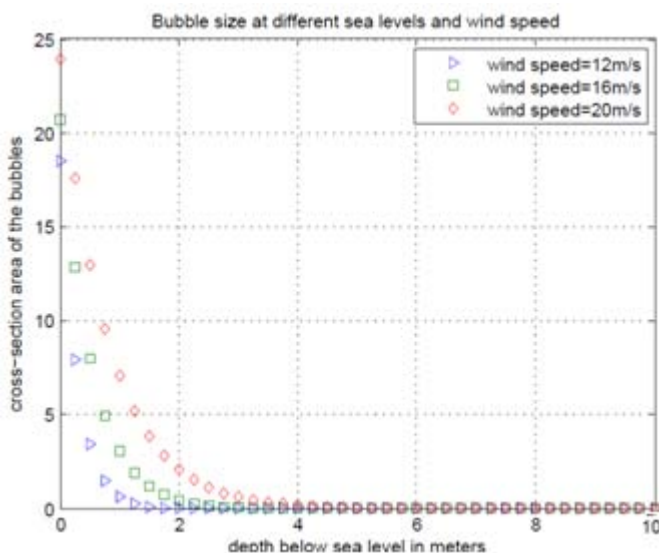


**Figure 3:** The Bubble size variation with the depth at different wind speed.

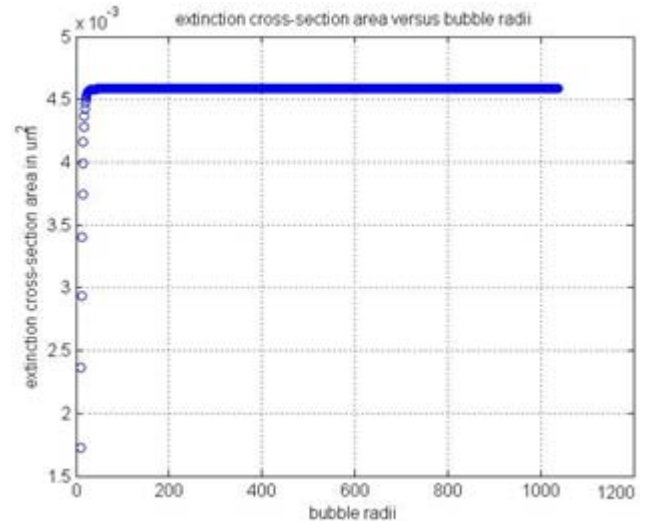


**Figure 4:** Extinction cross-section area of bubbles versus bubble radii

## 2. Conclusion

The bubble population, spectral shape, density are dependent on the range, depth, wind-speed. The scattering occurring in the acoustic frequency is due to the presence of the bubbles resulted from the wind-speed. Thus shallow water has potential attenuation causing factors and communication is a complex process here. The deep sea-communication is exhibited with OFC which is reliable but costly.

## 3. Future Scope

The channel characterization can be done more precisely considering the values for the parameter as dynamic and a more dynamic nature of the channel can be seen. The advances technology with ability of procuring the changing nature of sea-surface can estimate more accurately.

## References

- [1] Guy V. Norton and J. C. Novarini, "On the relative role of sea-surface roughness and bubble plumes in shallow water propagation in the low-kilohertz region," *J. Acoust. Soc. Am.*, Vol. 110, pp 2946-2955, December 2001.
- [2] J. C. Novarini, R. S. Keiffer, and G. V. Norton, "A model for variations in the range and depth dependence of the sound speed and attenuation induced by bubble clouds under wind-driven conditions," *IEEE J. Ocean Engineering*, Vol. 23, pp423-438, October 1998.
- [3] T. Elfouhaily, B. Chapron, K. Katsaros, and D. Vandemark, "A unified directional spectrum for long and short wind-driven waves," *JGR*, vol.102, no. C7, pp 15781-15796, 1997.
- [4] M. V. Hall, "A comprehensive model of wind-generated bubbles in the ocean and predictions of the effects on sound propagation at frequencies up to 40 kHz," *J. Acoust. Soc. Amer.*, vol. 86, pp. 1103-1116, 1989.
- [5] J. Wu, "Bubbles in the near-surface ocean: Their various structures," *J. Phys. Oceanogr.*, vol. 24, pp. 1955-1965, 1994.

- [6] J. C. Novarini and D. R. Bruno, "Effects of the sub-surface bubble layer on sound propagation," *J. Acoust. Soc. Amer.*, vol. 72, pp. 510–514, 1982.
- [7] D. E. Weston, "On the losses due to storm bubbles in oceanic sound transmission," *J. Acoust. Soc. Amer.*, vol. 86, pp. 1546–1553, 1988.
- [8] V. G. Bondur, and E. R. Sharkov, "Statistical properties of white caps on a rough sea," *Oceanology*, vol. 22, pp. 274–279, 1982.
- [9] J. Wu, "Bubble population and spectra in near-surface ocean: Summary and review," *J. Geophys. Res.*, vol. 86, pp. 453–463, 1981.
- [10] E.C. Monahan and M. Lu, "Acoustic relevant bubble assemblages and their dependence on meteorological parameters." *IEEE J. Ocean Engineering, Vol. 15, pp 340-349, 1990.*
- [11] S. A. Thorpe, "On the clouds of bubbles formed by breaking waves in deep water and their role in the air-sea gas transfer," *Philos. Trans. R.Soc. London Ser. A*, vol. 304, pp. 155–210, 1982.
- [12] R. C. Johnson and B. D. Cooke, "Bubble population and spectra in coastal waters: a photographic approach," *J. Geophys. Res.*, vol. 84, pp. 3761–3766, 1979.
- [13] H. Medwin and N. Breitz, "Ambient and transient bubble spectral densities in quiescent seas and under spilling breakers," *J. Geophys. Res.*, vol. 94, pp. 12751–12759, 1989
- [14] M. Y. Su, R. Burge, and J. Cartmill, "Measurements of near-surface microbubble density during SWADE," unpublished.